Structural Properties of $M(dmit)_2$-Based (M = Ni, Pd, Pt; $dmit^{2-}$ = 2-Thioxo-1,3-dithiole-4,5-dithiolato) Molecular Metals. Insights from Density Functional Calculations

Angela Rosa,*,† Giampaolo Ricciardi,† and Evert Jan Baerends*,‡

Dipartimento di Chimica, Università della Basilicata, Via N. Sauro, 85, 85100 Potenza Italy, and Afdeling Theoretische Chemie, Vrije Universiteit, De Boelelaan 1083, 1081 HV Amsterdam, The Netherlands

Received April 24, 1997

The bonding between two $M(dmit)_2$ monomers (M = Ni, Pd, Pt) in the stacks that are characteristic for the crystal structure of these compounds has been analyzed, using decomposition of the interaction energy in steric repulsion, electron pair bond formation, and donor−acceptor interactions. Atom over atom (eclipsed) stacking may occur if two conditions are met: (a) The HOMO to LUMO excitation energy should be small enough so that these singly occupied orbitals may both form an electron pair bond with their partner on the adjacent monomer. The HOMO and LUMO both being ligand based, the electron pair bonds are between the ligands and not between the metals. (b) The bending away of the ligand systems so as to relieve the steric hindrance should not cost too much energy. These circumstances prevail in $Pt(dmit)_2$, where relativistic effects increase the stability of the eclipsed conformation by enhancing the acceptor capability of the virtual orbitals with 6s, 7s, and $6p_z$ character on the metal for electron donation out of the occupied adjacent d_{z^2}. In $Ni(dmit)_2$ both the excitation energy is somewhat higher and the bending is more unfavorable; consequently, it does not exhibit the eclipsed stacking pattern. Slipping is another way to relieve the steric repulsion between adjacent monomers. The electron pair bonds are broken in that case, but sufficient donor−acceptor interactions between the two ligand systems remain to make this a viable alternative for $Ni(dmit)_2$. $Pd(dmit)_2$ is in between and may adopt either eclipsed or slipped configurations.

Introduction

The molecular charge transfer salts $[donor]_x[M(dmit)_2]$ (M = Ni, Pd, Pt; $0 < x < 1$), where the donor species is an inorganic or organic cation, are receiving considerable interest[1] owing to the structural similarity of the $M(dmit)_2$ acceptor unit with the organic isolobal analog BEDT-TTF, with its proven ability to form both molecular metals and superconductors.[2] They show a large variety of stoichiometries and structural and physical properties depending on the nature of the cation and on the nature of the metal in the $M(dmit)_2$ units. Most of the $M(dmit)_2$ salts investigated have structures with 1D or quasi 1D stacks of $M(dmit)_2$ molecules, which can be expected to provide the best conducting direction in the crystal. The features of the stacking pattern differ from one compound to another, the most usual structural motifs being the following (see Chart 1): (i) a sequence of approximately equidistant monomeric units **1**; (ii) a sequence of weak dimers ("diads") **2**; (iii) a sequence of monomeric and dimeric units **3**; (iv) a sequence of dimers **4**. Although it is hard to make a consistent classification of this wide variety of structural motifs in terms of stoichiometry, nature of the cation, and nature of the metal in the $M(dmit)_2$ units, some trends are apparent. Whatever the cation is, nickel salts generally form stack structures containing weak dimers (type **2**) or nearly equidistant monomers (type **1**), where the monomeric units lie at a distance (3.4−3.7 Å) which prevents effective Ni···Ni interactions.[3−6] Platinum, on the other hand, tends to form structures containing dimers where the Pt−Pt distance ranges from 2.9 to 3.1 Å.[3b,4f,6d,7] The palladium salts exhibit intermediate behavior, forming either structures containing

Chart 1

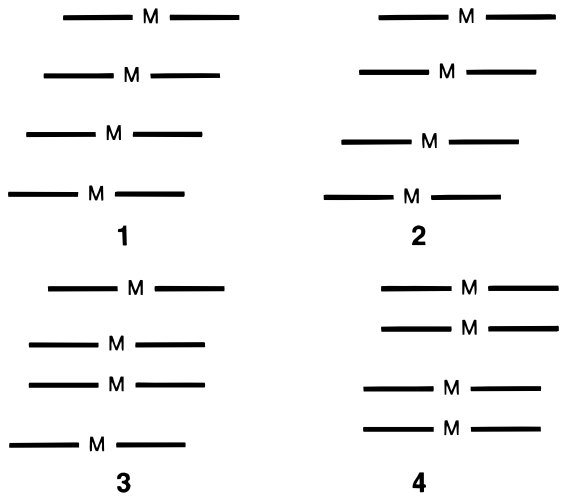

† Università della Basilicata.
‡ Vrije Universiteit.

(1) For a review, see: Cassoux, P.; Valade, L.; Kobayashi, H.; Kobayashi, A.; Clark, R. A.; Underhill, A. E. *Coord. Chem. Rev.* **1991**, *110*, 115.
(2) (a) Ferraro, J. M.; Williams, J. M. In *Introduction to Synthetic Electrical Conductors*; Academic Press: New York, 1987; pp 1−327. (b) Aldissi, M., Ed. Proceedings of the International Conference on Science and Technology of Synthetic Metals. *Synth. Met.* **1988**, *17*, A1−A528, B1−B666; **1989**; *28*, C1−C886, D1−D740; **1989**, *29*, E1−E744, F1−F752; (c) Saito, G., Kagoshima, S., Eds. *The Physics and Chemistry of Organic Superconductors*; Springer Proceedings in Physics; Springer Verlag: Berlin, 1990; Vol. 51, pp 1−476.

S0020-1669(97)00452-7 CCC: $15.00
Published on Web 02/24/1998

dimers with Pd−Pd bond lengths in the range 3.0−3.2 Å[3a,4d,f,5e,8] or sometimes stack structures of type **1**.[9]

The elements of a sequence, which may be monomers, dimers, or "diads", show similar overlap modes in the salts of M(dmit)$_2$ (M = Ni, Pd, Pt) series. They are in fact slipped either along the *x*, *y* axes or along any intermediate axis, the slipping angle α (the angle formed between the molecular symmetry axis and the stacking direction) ranging from 18 to 49°.

A slipped overlap mode is also adopted by the monomers forming the weak dimers of Ni salt structures. By contrast, the monomers forming the dimers occurring in Pt and sometimes in Pd salt structures show invariably an overlap mode of the atom-over-atom type (eclipsed). In this case, however, the two M(dmit)$_2$ units assume a V-shaped geometry, the folding angle ϕ, i.e. the dihedral angle between the M(dmit) moieties in each M(dmit)$_2$ unit, ranging from ∼6 to ∼11.5°.[3a,b,4d,5e,6d,7,8]

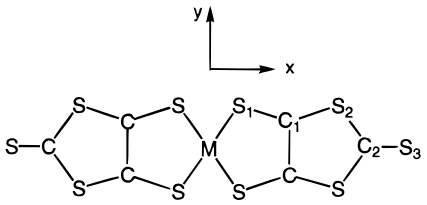

Figure 1. Atom labeling scheme for M(dmit)$_2$.

The structural trends just mentioned suggest that the cations have very little effect on the association modes of the M(dmit)$_2$ units along the stack, their role being restricted to the tuning of the fine details of the stacking pattern. The counterion was found to play a similarly minor role in small-ring (porphyrin) based 1D conductors.[10]

Previous theoretical studies, consisting mostly of extended Hückel tight-binding (EHTB) band structure calculations, have dealt with the conductive properties of these molecular charge transfer salts.[3f,4,8a,c,11] These investigations have helped to understand the structural and electronic factors controlling the Fermi surface topology and hence have greatly contributed to rationalize the electrical properties of these systems. The present theoretical investigation deals with the origin of the relevant structural features of the M(dmit)$_2$ stacks. Our aim is to answer some fundamental questions concerning the association modes of the acceptor units, such as the following: (i) why platinum tends to form [M(dmit)$_2$]$_2$ dimers, nickel generally forms stack structures containing weak dimers ("diads") or nearly equidistant monomers and palladium shows an intermediate behavior; (ii) why the monomeric units forming the one-dimensional chain or the "diads" adopt a slipped arrangement, whereas the monomeric units forming the dimers show invariably an atom-over-atom overlap mode; (iii) what is the origin and the relevance of the V-shaped distortion shown by the M(dmit)$_2$ units forming the dimers.

To answer the questions detailed above we have studied, using a density functional theoretical approach, electronic structure aspects of the interaction between two adjacent M(dmit)$_2$ (M = Ni, Pd, Pt) units forming [M(dmit)$_2$]$_2^n$ (n = 0, −1) dimeric moieties, at different metal−metal distances and in the following configurations (see Chart 2): (a) eclipsed, with the M(dmit)$_2$ monomers in their ground state planar (D_{2h}) geometry, **5**; (b) eclipsed, with the M(dmit)$_2$ monomers in a V-shaped (C_{2v}) geometry, **6**; (c) slipped along the *x* axis, **7**, along the *y* axis, **8**, and along the M−S$_1$ bond direction, **9** (see Figure 1 for notation).

We made extensive use of an energy decomposition scheme (see next section) that, combined with a fragment formalism, has proven an useful tool in the analysis of the interactions between neighboring units in the stacks forming metalloporphyrin based one-dimensional "molecular metals".[10]

(3) (a) Bousseau, M.; Valade, L.; Bruniquel, M.-F.; Cassoux, P.; Garbauskas, M.; Interrante, L. V.; Kasper, J. *Nouv. J. Chim.* **1984**, *8*, 3. (b) Bousseau, M.; Valade, L.; Legros, J.-P.; Cassoux, P.; Garbauskas, M.; Interrante, L. V. *J. Am. Chem. Soc.* **1986**, *108*, 1908. (c) Ulmet, J.-P.; Auban, P.; Khmou, A.; Valade, L.; Casoux, P. *Phys. Lett. A* **1985**, *113*, 217. (d) Johansen, I.; Bechgaard, K.; Rindorf, C.; Thorup, N.; Jacobsen, C. S.; Mortensen, K. *Synth. Met.* **1986**, *15*, 333. (e) Kato, R.; Kobayashi, H.; Kobayashi, A.; Naito, T.; Tamura, M.; Tajima, H.; Kuroda, H. *Chem. Lett.* **1989**, 1839. (f) Kobayashi, A.; Kato, R.; Kobayashi, H. In *The Physics and the Chemistry of Organic Superconductors*; Saito, G., Kagoshima, S., Eds.; Springer Verlag: Berlin, 1990; Vol. 51, pp 32−35. (g) Kobayashi, H.; Kato, R.; Mori, T.; Kobayashi, A.; Sasaki, Y. *Mol. Cryst. Liq. Cryst.* **1985**, *125*, 125. (h) Kobayashi, A.; Kato, R.; Kobayashi, H. *Synth. Met.* **1987**, *19*, 635.

(4) (a) Kobayashi, A.; Kim, H.; Sasaki, Y.; Kato, R.; Kobayashi, H. *Solid State Commun.* **1987**, *62*, 57. (b) Canadell, E.; Ravy, S.; Pouget, J.-P.; Brossard, L. *Solid Stae Commun.* **1990**, *75*, 633. (c) Kim, H.; Kobayashi, A.; Sasaki, Y.; Kato, R.; Kobayashi, H. *Chem. Lett.* **1987**, 1799. (d) Kobayashi, A.; Kim, H.; Sasaki, Y.; Kato, R.; Kobayashi, H.; Moriyama, S.; Nishio, Y.; Kajita, K.; Sasaki, W. *Chem. Lett.* **1987**, 1819. (e) Kato, R.; Kobayashi, H.; Kim, H.; Kobayashi, A.; Sasaki, Y.; Mori, T.; Inokuchi, H. *Chem. Lett.* **1988**, 865. (f) Pomarède, B.; Garreau, B.; Malfant, I.; Valade, L.; Cassoux, P.; Legros, J.-P.; Audouard, A.; Brossard, L.; Ulmet, J.-P.; Doublet, M.-L.; Canadell, E. *Inorg. Chem.* **1994**, *33*, 3401. (g) Cornelissen, J. P.; Le Loux, R.; Jansen, J.; Haasnoot, J. G.; Reedijk, J.; Horn, E.; SPek, A. L.; Pomarède, B.; Legros, J.-P.; Reefman, D. *J. Chem. Soc., Dalton Trans.* **1992**, 2911. (h) Canadell, E.; Rachidi, E. I.; Ravy, S.; Pouget, J.-P.; Brossard, L.; Legros, J.-P. *J. Phys. (Paris)* **1989**, *50*, 2967.

(5) (a) Kato, R.; Kobayashi, H.; Kobayashi, A.; Sasaki, Y. *Chem. Lett.* **1985**, 131. (b) Kobayashi, H.; Kato, R.; Kobayashi, A.; Sasaki, Y. *Ibid.* **1985**, 535. (c) Strzelecka, H.; Vicente, R.; Ribas, J.; Legros, J.-P.; Cassoux, P.; Petit, P.; André, J.-J. *Polyhedron* **1991**, *10*, 687. (d) Sakamoto, Y.; Matsubayashi, G.; Tanaka, T. *Inorg. Chim. Acta* **1986**, *113*, 137. (e) Kobayashi, A.; Kim, H.; Sakaki, Y.; Moriyama, S.; Nishio, Y.; Kajita, K.; Sasaki, W.; Kato, R.; Kobayashi, H. *Synth. Met.* **1988**, *27*, B339. (f) Kajita, K.; Nishio, Y.; Moriyama, S.; Kato, R.; Kobayashi, H.; Sasaki, W. *Solid State Commun.* **1988**, *65*, 361. (g) Kobayashi, H.; Kato, R.; Kobayashi, A.; Mori, T.; Inokuchi, H.; Nishio, Y.; Kajita, K.; Sasaki, W. *Synth. Met.* **1988**, *27*, A289.

(6) (a) Kato, R.; Mori, T.; Kobayashi, A.; Sasaki, Y.; Kobayashi, H. *Chem. Lett.* **1984**, 1819. (b) Kato, R.; Kobayashi, H.; Kim, H.; Kobayashi, A.; Sasaki, Y.; Mori, T.; Inokuchi, H. *Synth. Met.* **1988**, *27*, B359. (c) Valade, L.; Legros, J.-P.; Legros, C.; Tejel, B.; Pomarède, B.; Garreau, B.; Bruniquel, M.-F.; Cassoux, P.; Ulmet, J.-P.; Audouard, A.; Brossard, L. *Synth. Met.* **1991**, *42*, 2268. (d) Tejel, B.; Pomarède, B.; Legros, C.; Valade, L.; Cassoux, P.; Ulmet, J.-P. *Chem. Mater.* **1989**, *1*, 578. (e) Cornelissen, J. P.; Müller, E.; Vaassens, P. H. S.; Haasnoot, J. G.; Reedijk, J.; Cassoux, P. *Inorg. Chem.* **1992**, *31*, 2241. (f) Valade, L.; Legros, J.-P.; Bousseau, M.; Cassoux, P.; Garbauskas, M.; Interrante, L. V. *J. Chem. Soc., Dalton Trans.* **1985**, 783.

(7) (a) Kobayashi, A.; Sasaki, Y.; Kato, R.; Kobayashi, H. Chem. Lett. 1986, 387. (b) Kobayashi, A.; Miyamoto, A.; Kobayashi, H.; Clark, A.; Underhill, A. E. *J. Mater. Chem.* **1991**, *1*, 827. (c) Garreau, B.; Pomarède, B.; Cassoux, P.; Legros, J.-P. *J. Mater. Chem.* **1993**, *3*, 315.

(8) (a) Kobayashi, A.; Kim, H.; Sasaki, Y.; Murata, K.; Kato, R.; Kobayashi, H. *J. Chem. Soc., Faraday Trans.* **1990**, *86*, 361. (b) Legros, J.-P.; Valade, L.; Cassoux, P. *Synth. Met.* **1988**, *27*, B347. (c) Underhill, A. E.; Clark, R. A.; Marsden, I.; Allan, M.; Friend, R. H.; Tajima, H.; Naito, T.; Tamura, M.; Kuroda, H.; Kobayashi, A.; Kobayashi, H.; Canadell, E.; Ravy, S.; Pouget, J.-P. *J. Phys.: Condens. Matter* **1991**, *3*, 933. (d) Kobayashi, A.; Kobayashi, H.; Miyamoto, A.; Kato, R.; Clark, R. A.; Underhill, A. E. *Chem Lett.* **1991**, 2163.

(9) Legros, J.-P.; Valade, L. *Solid State Commun.* **1988**, *68*, 599.

(10) (a) Rosa, A.; Baerends, E. J. *Inorg. Chem.* **1992**, *31*, 4717. (b) Rosa, A.; Baerends, E. J. *Inorg. Chem.* **1993**, *32*, 5075.

(11) (a) Canadell, E.; Rachidi, I. E.-I.; Ravy, S.; Pouget, G.-P.; Brossard, L.; Legros, J.-P. *J. Phys. Fr.* **1989**, *50*, 1521. (b) Doublet, M.-L.; Canadell, E.; Pouget, J.-P.; Yagubskii, E. B.; Ren, J.; Whangbo, M.-H. *Solid State Commun.* **1994**, *88*, 699. (c) Garrau, B.; Pomaréde, B.; Faulmann, C.; Fabre, J.-M.; Cassoux, P.; Legros, J.-P. *C. R. Acad. Sci. Paris, Ser. II* **1991**, *313*, 509. (d) Vainrub, A.; Canadell, E.; Jérome, D.; Bernier, P.; Nunes, T.; Bruniquel, M.-F.; Cassoux, P. *J. Phys. Fr.* **1990**, *51*, 2465. (e) Brossard, L.; Canadell, E.; Valade, L.; Cassoux, P. *Phys. Rev. B* **1993**, *47*, 1647.

Chart 2

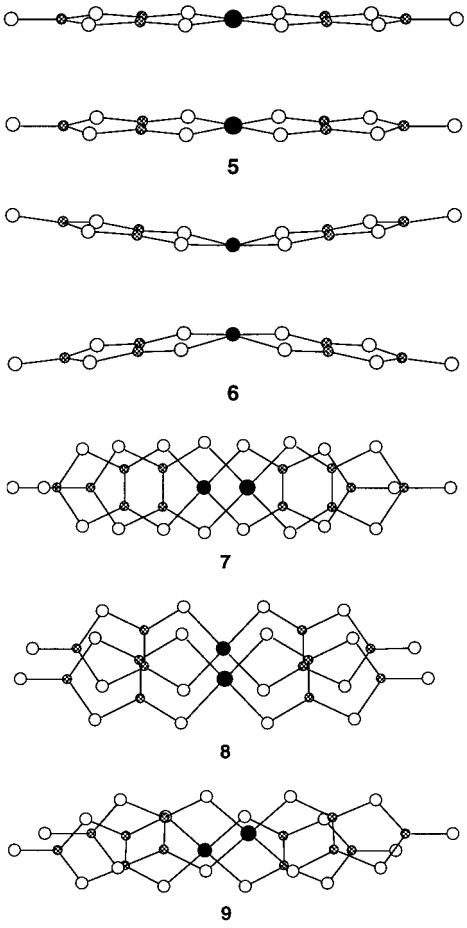

Methods

General Procedures. The calculations reported in this paper are based on the Amsterdam DF program package[12] characterized by the use of a density fitting procedure to obtain accurate Coulomb and exchange potentials in each SCF cycle,[12d] by accurate and efficient numerical integration of the effective one-electron Hamiltonian matrix elements[12e,f] and by the possibility to freeze core orbitals.[12a]

A double-ζ STO basis set augmented by a single STO d orbital was employed for sulfur and carbon atoms. The *n*d, $(n + 1)$s, and $(n + 1)$p shells of nickel, palladium, and platinum were represented by a triple-ζ basis.[12g,h] The cores (Ni, 1s−2p; Pd, 1s−4p; Pt, 1s−5p; C, 1s; S, 1s−2p) have been kept frozen.

The Vosko−Wilk−Nusair parametrization[13] of the electron gas data has been used for the local-density approximation (LDA) for the exchange-correlation energy and potential. The energies included Becke's[14] nonlocal corrections to the local expression of the exchange energy and Perdew's[15] nonlocal corrections to the local expression of correlation energy. The nonlocal corrections were added as a perturbation to the LDA energies (NL-P level).

The relativistic effects, which are important when heavy atoms, such as palladium and platinum are involved, were taken into account using the quasi-relativistic method (QR).[16] In this method, changes in the density induced by the first-order Hamiltonian are taken into account all orders of α^2 whereas operators in the Hamiltonian to second and higher orders are neglected.

We have first performed calculations on $Ni(dmit)_2$, $Pd(dmit)_2$, and $Pt(dmit)_2$ isolated molecules using the experimental geometry (see refs 3b, 8a, and 3b, respectively), with appropriate averaging of bond angles and bond lengths to maintain D_{2h} symmetry. The coordinate system used in the calculations as well as the labeling of the nonequivalent atomic centers in the molecules are shown in Figure 1.

The dimeric units in the eclipsed configurations **5** and **6** have been built by superimposing two $M(dmit)_2$ units in a planar D_{2h} geometry (**5**) and in a V-shaped C_{2v} (**6**) geometry, respectively, at metal−metal distances in the range 2.5−3.9 Å. For the dimers in configuration **6** the folding angle ϕ was set to 11°.

The dimeric units in the slipped configurations **7**−**9** have been built up from two planar $M(dmit)_2$ molecules at the interplanar distances of 2.9, 3.1, 3.3, and 3.5 Å. The offset along the *x*, *y*, and $M-S_1$ bond axes are varied so as to allow the slipping angle α to span the range 0−50°.

Interaction Energy Analysis. For the neutral dimers, $[M(dmit)_2]_2$, we have made an extensive analysis of the bonding between the $M(dmit)_2$ fragments from which the dimers are built up. To this purpose the overall interaction energy, denoted hereafter as dimerization energy, ΔE_{dim}, which is defined as the energy difference between two $M(dmit)_2$ fragments in their ground state and the final dimer

$$\Delta E_{dim} = E([M(dmit)_2]_2) - 2E(M(dmit)_2) \quad (1)$$

is decomposed into a number of terms, according to a method that is an extension of the well-known decomposition scheme of Morokuma.[17]

The first term, ΔE^0, is obtained from the energy of the wave function ψ^0, which is constructed as the antisymmetrized (*A*) and renormalized (*N*) product of the wave functions ψ^A and ψ^B of the fragments A and B:

$$\psi^0 = NA\{\psi^A\psi^B\} \quad E^0 = \langle\psi^0|H|\psi^0\rangle$$

$$\Delta E^0 = E^0 - E^A - E^B = \Delta E_{elstat} + \Delta E_{Pauli}$$

$$E^A = \langle\psi^A|H^A|\psi^A\rangle \quad E^B = \langle\psi^B|H^B|\psi^B\rangle$$

ΔE^0, which is appropriately called the steric repulsion,[18−20] consists of two components. The first is the electrostatic interaction ΔE_{elstat} of the nuclear charges and unmodified electronic charge density of one fragment with those of the other fragment, both fragments being at their final positions. Usually ΔE_{elstat} is negative, i.e. stabilizing. The second component is the so-called exchange repulsion or Pauli repulsion, ΔE_{Pauli}.[21,22] This is essentially due to the antisymmetry requirement on the total wave function, or equivalently the Pauli principle, which leads to a depletion of electron density in the region of overlap between ψ^A and ψ^B and an increase in kinetic energy.[23] The Pauli repulsion comprises the three- and four-electron destabilizing

(12) (a) Baerends, E. J.; Ellis, D. E.; Ros, P. *Chem. Phys.* **1973**, *2*, 42. (b) Baerends, E. J.; Ros, P. *Int. J. Quantum Chem.* **1978**, *S12*, 169. (c) Fonseca Guerra, C.; Visser, O.; Snijders, J. G. te Velde, G.; Baerends, E. J. In *Methods and Techniques in Computational Chemistry*; Clemeni, E., Corongiu, C., Eds.; STEF: Cagliari, Italy, 1995; Chapter 8, p 305. (d) Krijn, J.; Baerends, E. J. *Fit Functions in the HFS-Method*; Internal report (in Dutch); Vrije Universiteit: Amsterdam, The Netherlands, 1984. (e) Boerrigter, P. M.; te Velde, G.; Baerends, E. J. *Int. J. Quantum Chem.* **1988**, *33*, 87. (f) te Velde, G.; Baerends, E. J. *J. Comput. Phys.* **1992**, *99*, 84. (g) Snijders, J. G.; Baerends, E. J.; Vernooijs, P. *At. Nucl. Data Tables* **1982**, *26*, 483. (h) Vernooijs, P.; Snijders, J. G.; Baerends, E. J. *Slater type basis functions for the whole periodic system*; Internal report; Vrije Universiteit: Amsterdam, The Netherlands, 1981.
(13) Vosko, S. H.; Wilk, L.; Nusair, M. *J. Can. J. Phys.* **1980**, *58*, 1200.
(14) (a) Becke, A. D. *J. Chem. Phys.* **1986**, *84*, 4524. (b) Becke, A. D. *Phys. Rev.* **1988**, *A38*, 3098.
(15) (a) Perdew, J. P. *Phys. Rev.* **1986**, *B33*, 8822. (b) Perdew, J. P. *Phys. Rev.* **1986**, *B34*, 7406.
(16) Ziegler, T.; Tschinke, V.; Baerends, E. J.; Snijders, J. G.; Ravenek, W. *J. Phys. Chem.* **1989**, *93*, 3050.
(17) Morokuma, K. *J. Chem. Phys.* **1971**, *55*, 1236.
(18) (a) Ziegler, T.; Tschinke, V.; Becke, A. *J. Am. Chem. Soc.* **1987**, *109*, 1351. (b) Ziegler, T.; Tschinke, V.; Ursenbach, C. *J. Am. Chem. Soc.* **1987**, *109*, 4825. (c) Ziegler, T.; Tschinke, V.; Verslius, L.; Baerends, E. J. *Polyhedron* **1988**, *7*, 1625.
(19) Ziegler, T.; Rauk, A. *Inorg. Chem.* **1979**, *18*, 1558.
(20) Ziegler, T.; Rauk, A. **1979**, *18*, 1755.
(21) Fujimoto, H.; Osamura, J.; Minato, T. *J. Am. Chem. Soc.* **1978**, *100*, 2965.
(22) Kitaura, K.; Morokuma, K. *Int. J. Quantum Chem.* **1976**, *10*, 325.
(23) Van den Hoek, P. J.; Kleyn, A. W.; Baerends, E. J. *Comments At. Molec. Phys.* **1989**, *23*, 93.

interactions between occupied orbitals and is responsible for the steric repulsion.

In addition to the steric term ΔE^0, which is usually repulsive at the equilibrium distance since the repulsive component ΔE_{Pauli} dominates, there are the attractive orbital interactions which enter when the wave function ψ^0 is allowed to relax to the fully converged ground-state wave function of the total molecule,ψ^{AB}. The energy lowering due to mixing of virtual orbitals of the fragments into the occupied orbitals is called the electronic orbital interaction energy $\Delta E_{\text{oi}} = E[\psi^{AB}] - E^0$. In the case of closed-shell fragments the orbital interaction term ΔE_{oi} accounts for the charge transfer (interactions between occupied and virtual orbitals of the separate fragments) and polarization (empty/occupied orbital mixing on one fragment). In the case of open-shell fragments ΔE_{oi}, in addition to the charge transfer and polarization energies, also contain the energy lowering connected to the formation of the electron pair bonds, i.e. the energy gained by pairing the open-shell electrons in the bonding combination of the orbitals. The ΔE_{oi} term, according to the decomposition scheme proposed by Ziegler,[24] which is very useful for purposes of analysis, may be broken up into contributions from the orbital interactions within the various irreducible representations Γ of the overall symmetry group of the system:

$$\Delta E_{\text{oi}} = \sum_{\Gamma} \Delta E(\Gamma) \tag{2}$$

This decomposition scheme of the ΔE_{oi} term has been extensively used in this paper to analyze the attractive contributions to the bonding in the $[M(dmit)_2]_2$ dimers.

Electron pair bonds, which occur in the case of strong dimerization (*vide infra*), may be handled using an open-shell fragment procedure[25] and require for the analysis of ΔE_{oi} term a lowering of the symmetry of the systems. Thus, the symmetry has been lowered from D_{2h} to C_{2v} in the case of the eclipsed dimers in the configurations **5** and **6** and from C_{2h} to C_2 in the case of the slipped dimers in configurations **7** and **8**.

There is a third contribution to the dimerization energy in the cases where the ground-state wave functions ψ^A and ψ^B of the fragments cannot be used to calculate ΔE^0. The geometry of the fragments as they occur in the overall molecule can be different from the ground-state geometry. For instance, the $M(dmit)_2$ fragments in the dimers in configuration **6** show a sensible deviation from their D_{2h} equilibrium geometry. Also, the fragments may not be suitable for interactions in their ground-state electronic configuration. It may be then necessary to excite the fragments in a proper "valence state" which for strongly interacting $M(dmit)_2$ fragments is always the case. These are in fact not suitable for interaction in their closed-shell ground-state configuration (the dimerization is a forbidden reaction). As it will be shown later, strongly interacting $M(dmit)_2$ units form invariably two genuine electron pair bonds involving the HOMO's and LUMO's on the interacting fragments. The final dimer can be viewed as originating from two open-shell fragments in which the HOMO and LUMO on fragment A are singly occupied by α-spin electrons and the HOMO and LUMO on fragment B are singly occupied by β-spin electrons (see Scheme 1).

In this case we excite one electron from the HOMO to the LUMO in each $M(dmit)_2$ unit and use for the energy analysis a method developed for calculations from open-shell fragments.[25] In order to allow the electrons in the HOMO and LUMO orbitals of each fragment to pair up in the bonding $HOMO^+$ and $LUMO^+$ molecular orbitals, we define the wave functions ψ^A and ψ^B of the fragments A and B from which ψ^0 is constructed as

$$\psi^A = |(\text{closed shell})_A \cdot \varphi^{\text{HOMO}}\alpha\varphi^{\text{LUMO}}\alpha|$$

and

$$\psi^B = |(\text{closed shell})_B \cdot \varphi^{\text{HOMO}}\beta\varphi^{\text{LUMO}}\beta|$$

(24) Ziegler, T.; Rauk, A. *Theoret. Chim. Acta* **1977**, *46*, 1.
(25) Bickelhaupt, F. M.; Nibbering, N. M. M.; van Wezenbeek, E. M.; Baerends, E. J. *J. Phys. Chem.* **1992**, *96*, 4864.

Scheme 1

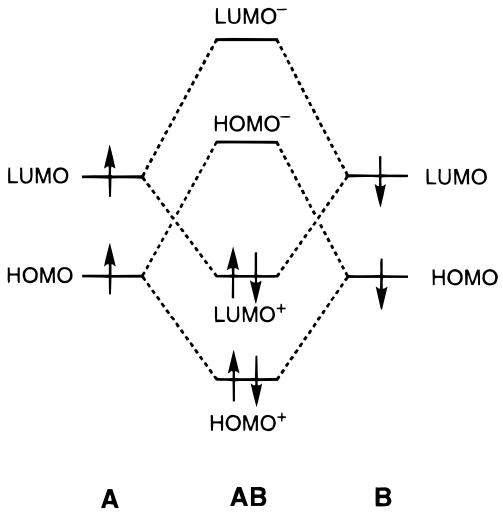

The energy required to prepare the fragments for interaction by changing the geometry and/or the electron configuration is referred to as preparation energy ΔE_{prep}. The wave functions ψ^A and ψ^B that are used to construct ψ^0 and to calculate E^0 now correspond to the prepared fragments.

We thus have

$$\Delta E_{\text{dim}} = \Delta E_{\text{prep}} + \Delta E^0 + \sum_{\Gamma} \Delta E(\Gamma) \tag{3}$$

This completes the definition of the energy terms displayed in the tables reported in this paper. For the monoanionic dimers, $[M(dmit)_2]_2^-$, the above bonding energy analysis has not been performed. We have restricted ourselves to the computation of the ΔE_{dim} defined, according to eq 1, as the energy difference between two $M(dmit)_2$ fragments in their ground state and the final ionic dimer.

Monomer Electronic Structure

The electronic structure of $M(dmit)_2$ complexes, unlike that of the parent metal bis(dithiolene) complexes, $M(bdt)_2$, for which a number of MO calculations have been reported, has never been investigated in detail. Actually, the nature and energy of the HOMO and LUMO is all that is known about the electronic structure of these systems. Only these orbitals have been considered since they were assumed to give rise to the relevant part of the electronic band structure of the $M(dmit)_2$-based salts. Since however, besides the HOMO and LUMO, many other MOs of the interacting monomers may play a role in determining the electronic and structural features of the dimeric units,[11] a more exhaustive description of the electronic structure of the isolated molecules is called for.

To this purpose, an atomic orbital population analysis of the ground-state one-electron levels is given in Table 1 for the series $Ni(dmit)_2$, $Pd(dmit)_2$, and $Pt(dmit)_2$. All the $M(dmit)_2$ molecules of the series have a closed-shell ground state, the HOMO being invariably the $4b_{1u}$ which is an almost pure p_π ligand orbital and lies in all systems at the same energy. This orbital is known to play, together with the LUMO, which also has predominantly ligand character (both are built from in-phase and out-of-phase combinations of π orbitals on the dmit ligand), a crucial role in the conductive properties of the $[donor]_x[M(dmit)_2]$ salts.

Concerning the metal *n*d orbitals, we note that in the level pattern of the $M(dmit)_2$ (M = Ni, Pd, Pt) molecules one easily recognizes the pseudo-square-planar environment of the $(nd)^8$ M, leading to a set of occupied d derived orbitals well below a vacant d_{xy} orbital ($8b_{1g}$) strongly destabilized by σ-antibonding interaction with sulfur lone pairs. As inferred from the

Table 1. Percentage Contribution of Individual Atoms to Selected Orbitals[a] (Based on Mulliken Population Analysis per MO) of $M(dmit)_2$ (M = Ni, Pd, Pt)[b]

		ϵ (eV)	M	S_1	S_2	S_3	C_1	C_2
$8b_{1g}$	$Ni(dmit)_2$	−4.68	35.0 ($3d_{xy}$)	53.0	0.0	7.0	5.0	0.0
	$Pd(dmit)_2$	−4.34	33.0 ($4d_{xy}$)	55.0	3.0	4.0	3.0	2.0
	$Pt(dmit)_2$	−4.21	33.0 ($5d_{xy}$)	52.0	4.0	5.0	4.0	2.0
$5b_{2g}$	$Ni(dmit)_2$	−5.34	13.0 ($3d_{xz}$)	52.0	5.0	10.0	18.0	2.0
	$Pd(dmit)_2$	−5.37	9.0 ($4d_{xz}$)	54.0	6.0	11.0	17.0	3.0
	$Pt(dmit)_2$	−5.41	10.0 ($5d_{xz}$)	53.0	6.0	11.0	17.0	3.0
$4b_{1u}$	$Ni(dmit)_2$	−6.10	2.0 ($4p_z$)	24.0	20.0	28.0	23.0	3.0
	$Pd(dmit)_2$	−5.98	3.0 ($5p_z$)	27.0	18.0	32.0	21.0	0.0
	$Pt(dmit)_2$	−6.03	2.0 ($6p_z$)	30.0	19.0	27.0	23.0	1.0
$3b_{3g}$	$Ni(dmit)_2$	−6.47	58.0 ($3d_{yz}$)	27.0	11.0	0.0	4.0	0.0
	$Pd(dmit)_2$	−6.78	34.0 ($4d_{yz}$)	41.0	20.0	0.0	5.0	0.0
	$Pt(dmit)_2$	−6.69	36.0 ($5d_{yz}$)	40.0	19.0	0.0	5.0	0.0
$7b_{2u}$	$Ni(dmit)_2$	−6.64	0.0	4.0	8.0	84.0 ($4p_y$)	0.0	4.0
	$Pd(dmit)_2$	−6.41	0.0	2.0	6.0	86.0 ($4p_y$)	3.0	3.0
	$Pt(dmit)_2$	−6.59	0.0	4.0	10.0	84.0 ($4p_y$)	0.0	2.0
$7b_{1g}$	$Ni(dmit)_2$	−6.68	2.0 ($3d_{xy}$)	2.0	10.0	83.0 ($4p_y$)	0.0	3.0
	$Pd(dmit)_2$	−6.47	1.0 ($4d_{xy}$)	2.0	8.0	85.0 ($4p_y$)	2.0	2.0
	$Pt(dmit)_2$	−6.66	2.0 ($5d_{xy}$)	1.0	9.0	83.0 ($4p_y$)	2.0	3.0
$11a_{1g}$	$Ni(dmit)_2$	−6.69	94.0 ($3d_{z^2}$, 4s)	6.0	0.0	0.0	0.0	0.0
	$Pd(dmit)_2$	−7.23	81.0 ($4d_{z^2}$, 5s)	19.0	0.0	0.0	0.0	0.0
	$Pt(dmit)_2$	−7.28	85.0 ($5d_{z^2}$, 6s)	12.0	3.0	0.0	1.1	2.8
$4b_{2g}$	$Ni(dmit)_2$	−6.80	29.0 ($3d_{xz}$)	7.0	25.0	34.0	4.0	1.0
	$Pd(dmit)_2$	−6.77	13.0 ($4d_{xz}$)	13.0	25.0	45.0	2.0	2.0
	$Pt(dmit)_2$	−6.86	15.0 ($5d_{xz}$)	12.0	29.0	40.0	3.0	2.0
$2a_{1u}$	$Ni(dmit)_2$	−7.27		60.0	37.0	0.0	3.0	0.0
	$Pd(dmit)_2$	−7.38		59.0	38.0	0.0	2.0	0.0
	$Pt(dmit)_2$	−7.41		55.0	43.0	0.0	2.0	0.0
$3b_{1u}$	$Ni(dmit)_2$	−7.60	2.0 ($4p_z$)	40.0	17.0	29.0	6.0	6.0
	$Pd(dmit)_2$	−7.38	2.0 ($5p_z$)	41.0	15.0	31.0	5.0	6.0
	$Pt(dmit)_2$	−7.46	2.0 ($6p_z$)	40.0	19.0	32.0	3.0	4.0
$10a_{1g}$	$Ni(dmit)_2$	−7.86	80.0 ($3d_{x^2-y^2}$, d_{z^2})	15.0	0.0	0.0	5.0	0.0
	$Pd(dmit)_2$	−8.49	67.0 ($4d_{x^2-y^2}$, d_{z^2})	22.0	0.0	0.0	6.0	0.0
	$Pt(dmit)_2$	−8.44	65.0 ($5d_{x^2-y^2}$, d_{z^2})	25.0	0.0	0.0	10.0	0.0
$3b_{2g}$	$Ni(dmit)_2$	−7.92	52.0 ($3d_{xz}$)	15.0	7.0	14.0	7.0	5.0
	$Pd(dmit)_2$	−8.55	63.0 ($4d_{xz}$)	5.0	2.0	8.0	14.0	7.0
	$Pt(dmit)_2$	−8.54	57.0 ($5d_{xz}$)	10.0	3.0	11.0	13.0	6.0
$2b_{3g}$	$Ni(dmit)_2$	−8.12	28.0 ($3d_{yz}$)	18.0	50.0	0.0	4.0	0.0
	$Pd(dmit)_2$	−8.53	32.0 ($4d_{yz}$)	4.0	56.0	0.0	7.0	0.0
	$Pt(dmit)_2$	−8.42	30.0 ($5d_{yz}$)	4.0	57.0	0.0	9.0	0.0
$1b_{3g}$	$Ni(dmit)_2$	−9.19	11.0 ($3d_{yz}$)	41.0	29.0	0.0	19.0	0.0
	$Pd(dmit)_2$	−9.49	30.0 ($4d_{yz}$)	40.0	16.0	0.0	12.0	0.0
	$Pt(dmit)_2$	−9.46	30.0 ($5d_{yz}$)	42.0	15.0	0.0	13.0	0.0

[a] In the numbering of the MOs the core electrons and the Ni 3s and 3p valence electrons are not included. [b] On sulfur and carbon the contributing AO's are p_y in the b_{2u} type orbitals, p_z in the b_{2g}, b_{3g}, a_{1u}, and b_{1u}, and mostly $p_{x,y}$ with some s in the a_{1g} and b_{1g} ones.

populations in Table 1, the $8b_{1g}$ has actually more S_1 σ-lone pair character, with ca. 35% d_{xy} character. Most of the d_{xy} character occurs in fact in the low-lying $4b_{1g}$ and $5b_{1g}$ (not in Table 1), the latter being the bonding counterpart of the $8b_{1g}$. The large (∼6 eV) energy gap between the $8b_{1g}$ and the $5b_{1g}$, and the considerable population of the d_{xy} orbital in all members of the series (1.26, 1.24, and 1.18 e in Ni, Pd, and Pt, respectively), are indicative of a strong metal−ligand σ interaction.

As for the remaining d states, the d_{z^2} is found almost purely (more than 80%) in the $11a_{1g}$ which also contains some (n + 1)s contribution and a small admixture of dmit σ orbitals. The $d_{x^2-y^2}$ occurs mostly in the $10a_{1g}$ where it mixes with the d_{x^2} and dmit σ orbitals. The mixings that occur in a_{1g} type orbitals cause a charge transfer from the filled d_{x^2} and $d_{x^2-y^2}$ into the (n + 1)s orbital, whose population (0.39, 0.40, and 0.30 e in Ni, Pd, and Pt, respectively) comes however also from dmit σ orbitals.

Metal−dmit π interactions involve the d_{yz} and d_{xz} orbitals in b_{3g} and b_{2g} symmetry, respectively. The d_{yz} interacts with occupied dmit π orbitals. However, the spacing (∼2.7 eV) of the resulting π bonding/antibonding pair $1b_{3g}3b_{3g}$ is much smaller than that of the σ bonding/antibonding pair. A large d_{yz} percentage (∼30%) is found also in the $2b_{3g}$ where it accidentally mixes with a b_{3g} (π) orbital of the ligand mainly localized on S_2 atoms. Since the mixings that occur in b_{3g} type orbitals involve almost exclusively occupied dmit π orbitals, the charge depletion of the d_{yz} is negligible. The d_{xz} occurs mostly in the occupied $3b_{2g}$ and, to a sizable extent, also in the $4b_{2g}$ which is mainly an S_2 based ligand π orbital. The d_{xz} also interacts with a virtual dmit π orbital of b_{2g} symmetry, which is largely (∼65%) localized on the S_1 atoms. However, due to enery mismatch, the metal contribution to the resulting antibonding MO, the $5b_{2g}$, is quite low (∼10%). This S_1-based $5b_{2g}$ is the LUMO in the $M(dmit)_2$ series. The mixing of d_{xz} with the lowest empty b_{2g} dmit orbital results in a small but

not negligible π back-donation from the filled d_{xz} into the empty b_{2g} dmit orbital that amounts to 0.28, 0.22, and 0.26 e for Ni, Pd, and Pt, respectively.

As inferred from the energy values of the MOs listed in Table 1, the occupied metal states show a significant downward shift when going from Ni to Pd but change very little when going from Pd to Pt. One may also observe that in a bonding/antibonding pair (for instance the $1b_{3g}/3b_{3g}$ pair) the metal contribution in the upper level is usually largest in the case of Ni.

As for the ligand states, besides the $4b_{1u}$ HOMO and $5b_{2g}$ LUMO, there are two pairs of close-lying ligand states worth mentioning, the upper pair $7b_{2u}$ and $7b_{1g}$ and the lower pair $2a_{1u}$ and $3b_{1u}$. The $2a_{1u}$ and the $3b_{1u}$ are very suitable for interactions between monomers since they are composed, similar to the HOMO ($4b_{1u}$), of dmit p_π orbitals perpendicular to the molecular plane. The $7b_{2u}$ and the $7b_{1g}$ may play an important role in the lateral interactions, since they are composed of S_3 σ lone-pairs.

An important point to arise from the electronic structure of the M(dmit)$_2$ series is that all the MOs that involve the metal to a significant extent, except for the $8b_{1g}(d_{xy})$, are occupied. This implies that, in the eclipsed and in the slightly slipped [M(dmit)$_2$]$_2$ dimers, the well-known σ, π, and δ interactions present in typical metal−metal-bonded M_2L_8 compounds will mostly involve filled orbitals, a point to which we will return below.

Electronic Structure and Bonding in the Eclipsed [M(dmit)$_2$]$_2^n$ (n = 0, −1) Dimers

Orbital Interactions. We will first consider the electronic structure of the neutral [M(dmit)$_2$]$_2$ dimers in the metal-over-metal configurations **5** (planar monomers) and **6** (folded monomers). Although the folded dimers are built up from two M(dmit)$_2$ units in a V-shaped C_{2v} geometry, we may still use, to discuss the interactions between adjacent M(dmit)$_2$ molecules, the MOs of the D_{2h} planar monomers. The displacement of the metal out of the $(S_1)_4$ plane (pyramidalization) in the M(dmit)$_2$ units is small (∼0.2 Å), and the orbital energies and compositions for planar (D_{2h}) and non planar (C_{2v}) M(dmit)$_2$ units are thus very similar.

The most important interactions between strongly interacting (M−M distance = 2.9 Å) M(dmit)$_2$ units are shown in the diagrams of Figures 2−4 for the three dimers of the series in the two considered configurations. The significant point to arise from the electronic structure of the [M(dmit)$_2$]$_2$ dimers is that the dimerization of the M(dmit)$_2$ (M = Ni, Pd, Pt) units, either in the configuration **5** or **6**, is invariably accompanied by a LUMO$^+$/HOMO$^-$ crossing. The M−M distance at which the LUMO$^+$ ($14b_{3u}$) and the HOMO$^-$ ($15b_{1u}$) cross depends both on the metal and on the configuration of the dimers. As shown in Figure 5, in the folded dimers the LUMO$^+$ and the HOMO$^-$, which are actually the frontier orbitals, cross at M−M distances shorter than 3.3 Å, whatever the metal is. In the unfolded dimers this crossing occurs at much longer M−M distances, i.e. shorter than 3.7 Å in Ni and shorter than 3.9 Å in Pd and Pt. That the M(dmit)$_2$ units have to approach much closer in the folded dimers for the LUMO$^+$ and HOMO$^-$ to cross is a consequence of the ligand-based character of the HOMO and LUMO. The folding will therefore decrease the overlap. Upon folding, the overlap between the $5b_{2g}$ HOMOs and between the $4b_{1u}$ LUMOs is reduced indeed by about 50%. (The overlap of the HOMO on one monomer with the LUMO on the other is zero by symmetry.) The different splitting of the plus and minus combinations of these orbitals in the two configurations of the dimers is clearly visible in the diagrams of Figures 2−4. In the unfolded dimers the relatively strong orbital interaction

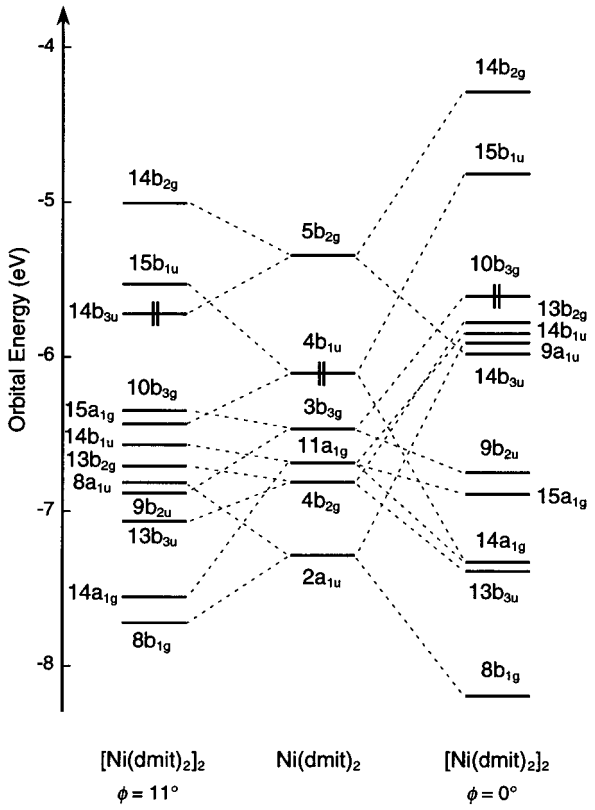

Figure 2. Orbital interaction diagram for [Ni(dmit)$_2$]$_2$ dimer (Ni−Ni distance = 2.9 Å) in the configurations **5** (ϕ = 0°) and **6** (ϕ = 11°).

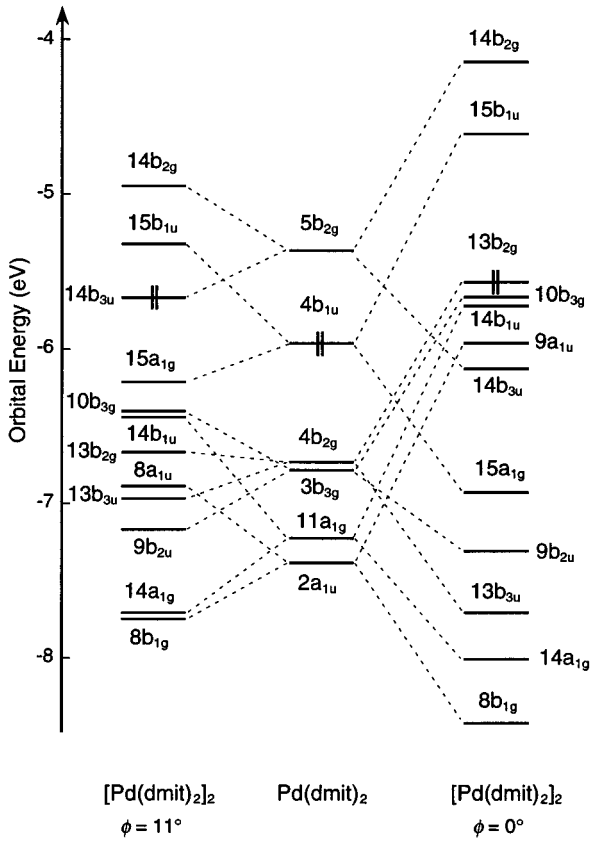

Figure 3. Orbital interaction diagram for [Pd(dmit)$_2$]$_2$ dimer (Pd−Pd distance = 2.9 Å) in the configurations **5** (ϕ = 0°) and **6** (ϕ = 11°).

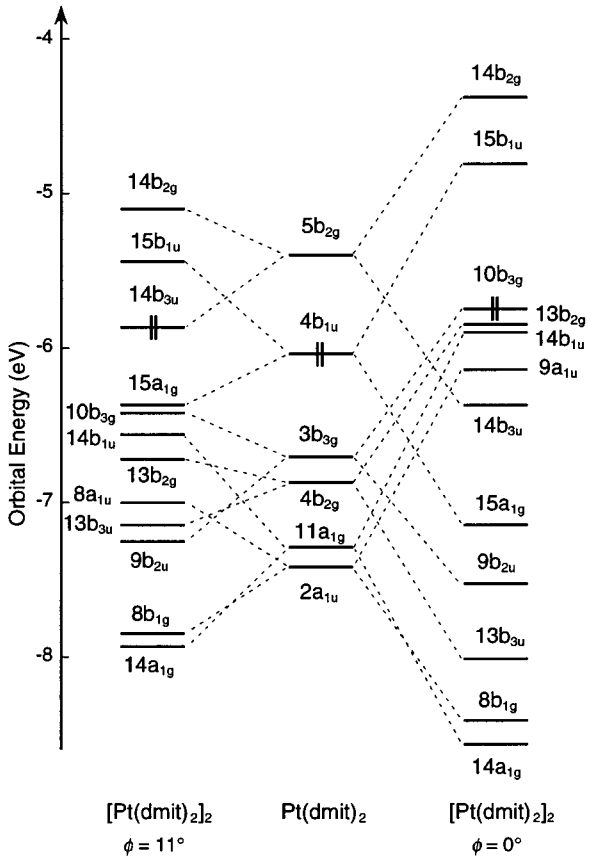

Figure 4. Orbital interaction diagram for $[Pd(dmit)_2]_2$ dimer (Pt−Pt distance = 2.9 Å) in the configurations **5** ($\phi = 0°$) and **6** ($\phi = 11°$).

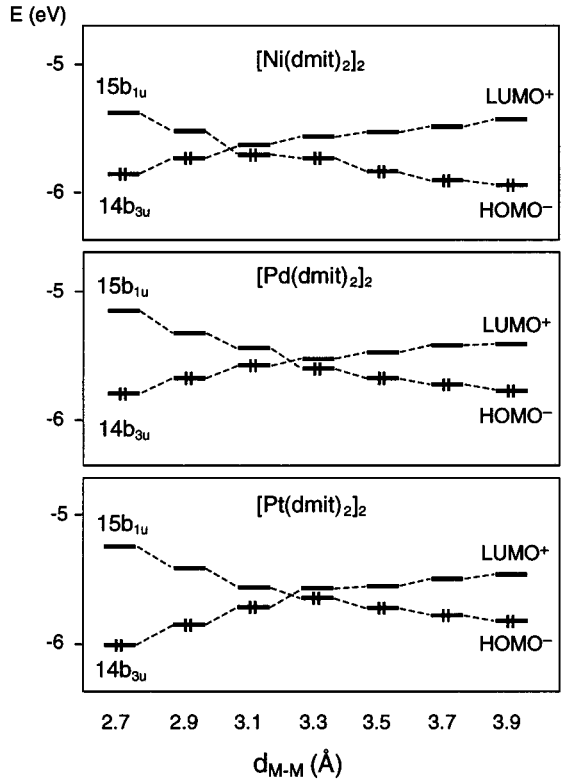

Figure 5. Energy of the frontier orbitals of $[M(dmit)_2]_2$ (M = Ni, Pd, Pt) dimers in the configuration **6** ($\phi = 11°$) at selected M−M distances.

stabilizes the $LUMO^+$ so that at short distances it is not the highest occupied level in the dimer (which it is in the folded dimers; see Figures 2−4). The $HOMO^-$ is the lowest unoccupied level in all dimers. In $[Ni(dmit)_2]_2$ and in $[Pt(dmit)_2]_2$ at M−M distances shorter than 3.1 and 3.3 Å, respectively, the highest occupied level becomes the $10b_{3g}$. In $[Pd(dmit)_2]_2$, at M−M distances shorter than 3.1 Å, the $13b_{2g}$ is the highest occupied level.

The occurrence of the $LUMO^+/HOMO^-$ crossing indicates that the dimerization of the $M(dmit)_2$ (M = Ni, Pd, Pt) units is a "forbidden" reaction which requires an activation energy. Since the HOMO/LUMO gap is small in all members of the series and decreases on going from Ni to Pt, the activation energy is expected to be small and to decrease in the same direction. The $M(dmit)_2$ fragments may be "prepared" for interaction by exciting one electron from the HOMO to the LUMO. It should be noticed that this excitation energy (that will contribute to the preparation energy term, ΔE_{prep}) is more than compensated by the formation of two genuine electron pair bonds, $4b_{1u} + 4b_{1u}$ ($HOMO^+$) and $5b_{2g} + 5b_{2g}$ ($LUMO^+$). These two electron pair bonds involve almost pure ligand orbitals, but there are no further ligand−ligand bonding interactions in the eclipsed dimers. Whatever the configuration of the dimers is, the ligand-based $2a_{1u}$ and $3b_{1u}$, which as noted above are very suitable for out-of-plane interactions, give rise in fact to four-electron two-orbital repulsive interactions, since both the bonding and antibonding derived levels are occupied. The overlap of these orbitals heavily depends on the configuration of the dimers, just like that of $5b_{2g}$ (HOMO) and $4b_{1u}$ (LUMO) π ligand orbitals, and decreases by more than 50% upon folding.

As far as the metal−metal interactions are concerned, most of them are between filled orbitals and can be classified as four-electron two-orbital repulsions. For the metal−metal δ and π bonding interactions this is just the case. A small M−M π bonding contribution arises from the occupation of the $LUMO^+$ orbital in the formation of one of the above mentioned electron pair bonds, since the $5b_{2g}$ (LUMO) orbitals has ∼10% of d_{xz} character.

As for the M−M σ interactions, they merit a more detailed discussion. The possibly σ bonding orbital $11a_{1g}$ has mainly metal d_{z^2} character in all members of the series (81−94%). The $11a_{1g}$ orbitals on adjacent monomers form + and − combinations of a_{1g} and b_{1u} symmetry, respectively, which as indicated in Figures 2−4 are both occupied, and therefore represent four-electron repulsion. However, there is a certain amount of donor−acceptor interaction between the occupied $11a_{1g}$-d_{z^2} of one monomer and suitable empty orbitals of the other monomer. One obvious acceptor orbital is the ligand-based $4b_{1u}$ (HOMO) orbital, more precisely the − combination $HOMO^-$ which is empty after the crossing with the $LUMO^+$. The $11a_{1g}^-$ combination forms primarily the $14b_{1u}$ orbitals, and the $HOMO^-$, the $15b_{1u}$ orbital, but due to mixing of these orbitals a non-negligible percentage of the $11a_{1g}^-$ (about 10% in the planar and 20% in the folded dimers) enters the $15b_{1u}$ orbital. This represents metal−ligand intermonomer donor−acceptor bonding. Metal−metal donor−acceptor bonding also occurs. In Pt, and to some extent in Pd, a M−M σ bond arises from mixing of the $11a_{1g}$-d_{z^2} with empty s and p metal orbitals on the adjacent monomer. These occur in high-lying virtual orbitals such as $15a_{1g}$ and $16a_{1g}$ (Pt 6s and 7s character) and $6b_{1u}$ (Pt $6p_z$ character). Donation of electrons from $11a_{1g}$-d_{z^2} to these AOs on the adjacent metal is equivalent to mixing of the − combinations of $15a_{1g}$, $16a_{1g}$, and $6b_{1u}$ into $14b_{1u}$. The actual amount of charge donation out of the $11a_{1g}$-d_{z^2} increases with shorter M−M distances and is rather metal dependent, being largest in $[Pt(dmit)_2]_2$. At the short distance of 2.9 Å the $11a_{1g}$ loses in Ni, Pd, and Pt unfolded dimers 0.10, 0.15, and 0.33 e

of which 0.08, 0.09, and 0.13 are acquired by the $4b_{1u}$. The rest, amounting to some 0.2 e in Pt, is donated to the virtual na_{1g} (6s, 7s) and nb_{1u} ($6p_z$) fragment orbitals. The na_{1g} fragment orbitals acquire an additional charge by mixing into a low-lying occupied b_{1u} (σ-ligand) dimer orbital. The charge depletion of the $11a_{1g}$ does not change substantially upon folding. The 6s, 7s, and 6p contribution to the $14b_{1u}$ (as well as to the higher $15b_{1u}$ and to the lower $13b_{1u}$) appears to be a clear relativistic effect that is manifest mostly in the Pt complexes. At the nonrelativistic level, in fact, the above mentioned mixings are irrelevant.

Addition of an electron, resulting in the monoanionic dimers $[M(dmit)_2]_2^-$, leaves the relevant features of the electronic structure, such as the ordering and composition of the MOs, practically the same. There are, however, significant effects on the bond between the M(dmit)$_2$ units. The unpaired electron will populate at large distance the LUMO$^+$ and at short distance, after the crossing, the HOMO$^-$. When the additional electron goes into the HOMO$^-$, as in the case of strongly dimerized systems, the attractive interaction arising from the $4b_{1u} + 4b_{1u}$ (HOMO$^+$) electron pair bond is partially destroyed and the bond between the M(dmit)$_2$ units is weakened. The partial occupation of the LUMO$^+$ that occurs in weakly dimerized systems causes on the contrary a strengthening of the bond between the M(dmit)$_2$ units, given the bonding nature of this orbital.

Energy Decomposition. From the electronic structure calculations on $[M(dmit)_2]_2^n$ ($n = 0, -1$) eclipsed dimers we have found that, irrespective of the conformation of the dimer, attractive interactions are provided by two genuine electron pair bonds, $4b_{1u} + 4b_{1u}$ and $5b_{2g} + 5b_{2g}$. In the monoanionic dimers, $[M(dmit)_2]_2^-$, the attractive interaction arising from the $4b_{1u} + 4b_{1u}$ electron pair bond is however partially destroyed. In the heavier element dimers, essentially in Pt, an additional attractive contribution stems from metal−metal donative σ interaction and from metal to ligand charge transfer. The remaining interactions are repulsive (four-electron two-orbital interaction).

Since the attractive interactions due to the electron pair bonds and the repulsive four-electron two-orbital interactions are larger the more effective the overlap is, one would expect that both these interactions will be enhanced when the dimerization is strong (short M−M distance) and/or the dimers are in the planar configuration **5** and will be reduced when the dimerization is weak (long M−M distance) and/or the dimers are in the folded configuration **6**. Therefore, which of the two configurations and which M−M distance would be adopted by the $[M(dmit)_2]_2^n$ ($n = 0, -1$) eclipsed dimers will depend on a delicate balance between the interactions just mentioned and would be unpredictable in the absence of a quantitative analysis of the contributions to the dimerization energy.

We have computed for both configurations of the $[M(dmit)_2]_2^n$ ($n = 0, -1$) dimers of the series the dimerization energies as a function of the M−M distance. For the neutral dimers, a quantitative energy analysis of the contributions of the dimerization energies has also been performed.

Let us discuss the formation of the $[M(dmit)_2]_2$ neutral dimers from two M(dmit)$_2$ units. The dimerization energies computed for the configurations **5** and **6** of the $[M(dmit)_2]_2$ dimers of the series are plotted as a function of the M−M distance in Figures 6 and 7, respectively. From the ΔE_{dim} curves displaed in Figure 6, it is apparent that the interaction of two M(dmit)$_2$ units to form a dimer in the configuration **5** is repulsive, although in Pd and Pt the ΔE_{dim} curves show a very shallow minimum around 3.5 Å. The shape of the ΔE_{dim} curves reflects the predominance of the repulsive contributions of ΔE^0 and ΔE_{prep}

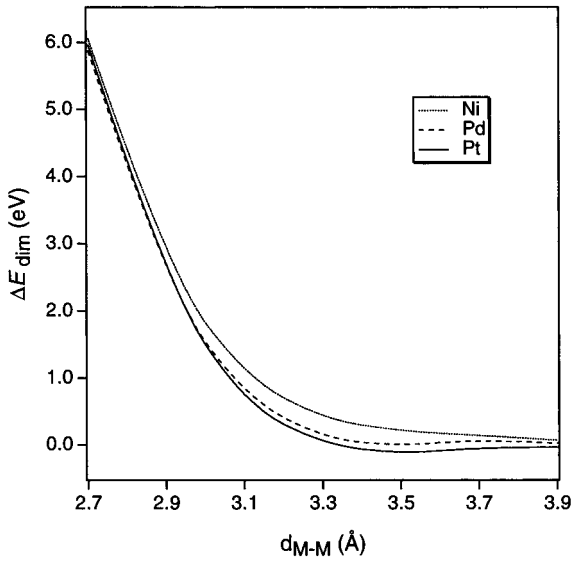

Figure 6. Dimerization energy, ΔE_{dim}, of M(dmit)$_2$ (M = Ni, Pd, Pt) units in the eclipsed configuration **5** as a function of the M−M distance.

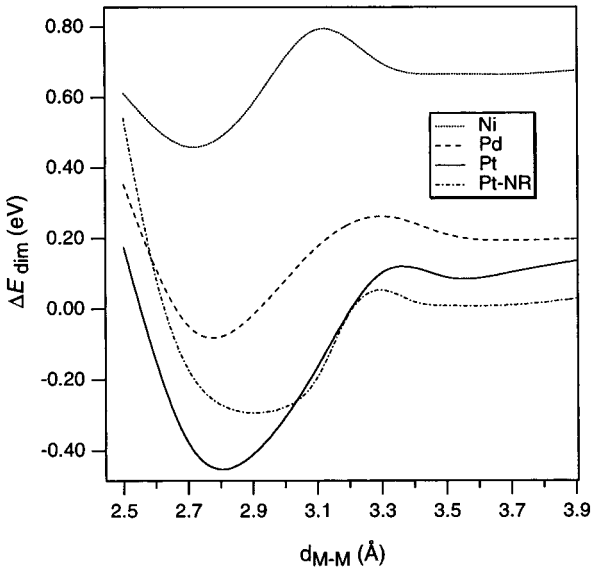

Figure 7. Dimerization energy, ΔE_{dim} of M(dmit)$_2$ (M = Ni, Pd, Pt) units in the eclipsed configuration **6** as a function of the M−M distance.

over the attractive orbital interaction ΔE_{oi} at all M−M distances (only at 3.5 Å in Pd and Pt, ΔE_{oi} is slightly larger). The destabilizing ΔE_{prep} term consists in the present case of planar monomers only of the excitation energy of one electron from the HOMO to the LUMO of the interacting M(dmit)$_2$ fragments. Since the HOMO$^-$/LUMO$^+$ crossing in the unfolded dimers already occurs at 3.5 Å in Ni and 3.7 Å in Pd and Pt dimers, ΔE_{prep} is a constant term consisting of this excitation energy for virtually all distance. [In the case of folded dimers, for which the HOMO$^-$/LUMO$^+$ crossing occurs at shorter distance, ΔE_{prep} at large distance consists of the bending energy, to which at shorter distance the excitation energy is added.] The important destabilizing contribution, however, is not ΔE_{prep} but is the ΔE^0 term, which strongly increases upon shortening of the distance. The repulsive ΔE_{Pauli} and attractive ΔE_{elstat} contributions to ΔE^0 exhibit the typical behavior of increasing in opposite directions upon shortening the distance, but ΔE_{Pauli} clearly dominates. At short interplanar distances, the Pauli repulsion term is strongly positive in all three dimers of the series, being largest in [Pt(dmit)$_2$]$_2$ due to the larger metal−metal repulsion. The attractive

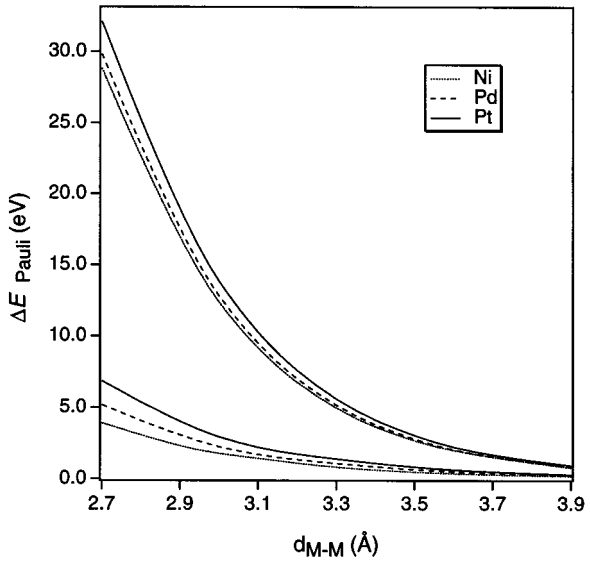

Figure 8. Pauli repulsion, ΔE_{Pauli}, of $[M(dmit)_2]_2$ (M = Ni, Pd, Pt) dimers in the eclipsed configurations **5** (upper curves) and **6** (lower curves) as a function of the M−M distance.

interaction term ΔE_{oi} also increases in all dimers upon decreasing the interplanar distance between the interacting $M(dmit)_2$ fragments but much less than the ΔE^0 term does, so it is the ΔE^0 term that determines the repulsive wall on the ΔE_{dim} curves plotted in Figure 6.

When looking at the ΔE_{dim} curves for the folded dimers displayed in Figure 7, we immediatley note that, at relatively short M−M distances, in all three dimers of the series, in place of the repulsive wall observed in the case of the unfolded dimers there is a minimum. Note that at large distance the dimerization energy does not go to zero since it comprises at all distances the folding energy of each of the two monomers. This is because we do not optimize the bending angle but keep it fixed at all distances. The bending energy is moderate in the case of $[Pd(dmit)_2]_2$ (0.27 eV) and $[Pt(dmit)_2]_2$ (0.24 eV) but substantial in case of $[Ni(dmit)_2]_2$ (0.73 eV). As a result, our folded $[Ni(dmit)_2]_2$ is unstable with respect to free monomers at all distances, $[Pd(dmit)_2]_2$ is moderately stable at the optimal M−M distance of ∼2.75 Å, $[Pt(dmit)_2]_2$ is very stable at the optimal M−M distance of ∼2.8 Å. The striking difference between the planar configuration (Figure 6) and folded configuration (Figure 7) is a direct consequence of the reduction of the Pauli repulsion between the ligands when they bend away from each other. This is apparent from Figure 8, where the ΔE_{Pauli} term is plotted as a function of the M−M distance for the configurations **5** and **6** of $[M(dmit)_2]_2$.

It is interesting to note that there is a barrier at ∼3.1 Å in the Ni ΔE_{dim} curve and at ∼3.3 Å in Pd and Pt, respectively. This is related to the symmetry-forbidden nature of the dimerization. As long as the $HOMO^-$ is occupied, there is a four-electron two-orbital destabilizing interaction that increases when the monomers approach each other. After the configuration change resulting in an occupied $LUMO^+$ the two bonds represented by $LUMO^+$ and $HOMO^+$ become stronger when the distance decreases, leading to the minima in the curves of Figure 7. These energetic effects can be followed in detail in the terms arising from the energy decomposition; cf. the Methods section. The ΔE_{prep} term for the folded configuration ($\phi = 11°$) will at distances shorter than 3.1 Å in Pd and Pt and 2.9 Å in Ni contain the excitation energy HOMO → LUMO. It therefore steps up at those distances (going to shorter distance). The excitation prepares the monomers for the formation of two electron pair bonds. The formation of these bonds is reflected clearly in a sharp rise at the same distances of the orbital interaction contributions in A_1 and B_1 symmetry, the ΔE^{A_1} and the ΔE^{B_1} energies, which are by far the largest contributions to ΔE_{oi}. [The two electron pair bonds, $4b_{1u} + 4b_{1u}$ and $5b_{2g} + 5b_{2g}$, occur in the A_{1g} and B_{3u} representations, respectively, but in the lower C_{2v} symmetry that is employed here A_{1g} reduces to A_1 and B_{3u} reduces to B_1.] The ΔE^{A_1} term is in all dimers sensibly larger than ΔE^{B_1} for the following reasons: (i) Owing to a larger overlap between the involved orbitals, the $4b_{1u} + 4b_{1u}$ ($HOMO^+$) electron pair bond provides a stronger energy contribution than the $5b_{2g} + 5b_{2g}$ ($LUMO^+$) does. (ii) The ΔE^{A_1} term contains an additional energy contribution arising from the occupied/virtual mixings occurring in this symmetry by the b_{1u} and a_{1g} type orbitals of the dimers. This additional energy contribution also causes the ΔE^{A_1} terms to be largest in Pt dimers where, as already pointed out, the occupied/virtual mixings are particularly effective.

The electron pair bonding energies, i.e. the ΔE^{A_1} and ΔE^{B_1} terms, are reduced by the folding, although ΔE^{A_1} rather less than ΔE^{B_1}. The reason is that the folding, by reducing the overlap of the largely ligand based $4b_{1u}$ and $5b_{2g}$ ($M(dmit)_2$ orbitals, weakens both the $HOMO^+$ and $LUMO^+$ bonds. The folding is still favorable since it reduces the total Pauli repulsion more than it weakens the electron pair bonds.

The ΔE^{A_1} term drops less than ΔE^{B_1} upon folding since the contribution arising from the occupied/virtual mixings occurred in b_{1u} and other type orbitals of the dimers is not reduced by the folding. It is this contribution that causes the ΔE^{A_1} term to be, just as in the unfolded dimers, largest in $[Pt(dmit)_2]_2$ where, due to relativistic effects, these occupied/virtual mixings are very strong. The influence of the relativistic effects on the stabilization of the ΔE^{A_1} term in $[Pt(dmit)_2]_2$ can be seen by comparing the relativistic and nonrelativistic ΔE^{A_1} values. According to our calculations, at 2.9 Å, for instance, the ΔE^{A_1} term is stabilized by 0.24 eV. In the corresponding Pd dimer the relativistic stabilization of the ΔE^{A_1} term only amounts to 0.04 eV, in line with the general trend of the relativistic effects going from 5d to 4d homologues. We may therefore argue that $[Pd(dmit)_2]_2$ differs from $[Pt(dmit)_2]_2$ in that the attractive orbital interactions are in the former less stabilizing mainly because of the poorer relativistic stabilization of the ΔE^{A_1} term. Thus, even in the well region of the ΔE_{dim} curve, the dimerization energy computed for $[Pd(dmit)_2]_2$ is quite small.

Turning now to the monoanionic dimers $[M(dmit)_2]_2^-$ of the series in the eclipsed configurations **5** and **6**, we point out that the dimerization energy of the monoanions defined as

$$\Delta E_{\text{dim}} = E([M(dmit)_2]_2^-) - 2E(M(dmit)_2)$$

is computed to be ∼4 eV more stabilizing than that of the corresponding neutral dimers. In this case, however, the dimerization energy does not correspond to the bond strength between the monomeric units because it also includes the energy gained when adding one electron to one if the two $M(dmit)_2$ units, which is computed to be ∼4 eV.

Considering first the $[M(dmit)_2]_2^-$ dimers in the planar configuration, we find that the ΔE_{dim} curves (not reported here) show, as in the case of the corresponding neutral dimers, a repulsive character. The addition of an electron does of course not diminish the Pauli repulsion responsible for the repulsion between the eclipsed planar monomers. We have therefore clearly identified the Pauli repulsion as the main reason for the $[M(dmit)_2]_2^n$ ($n = 0, -1$) dimers to never adopt the metal-over-metal configuratino **5**.

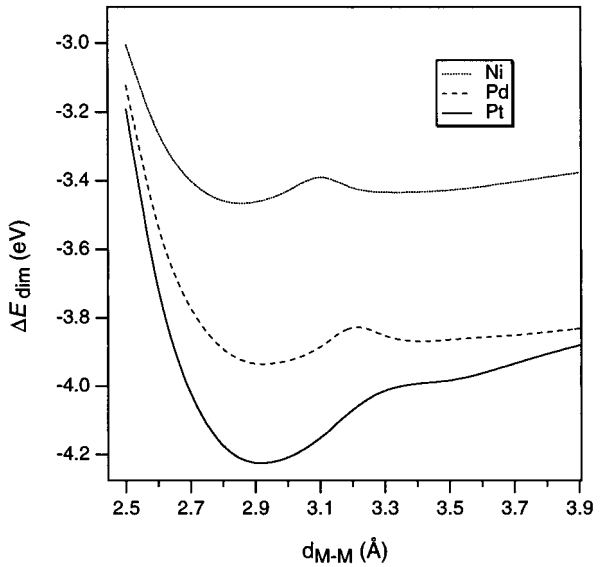

Figure 9. Dimerization energy, ΔE_{dim}, of $[M(dmit)_2]_2^-$ (M = Ni, Pd, Pt) dimers in the eclipsed configuration **6** as a function of the M−M distance.

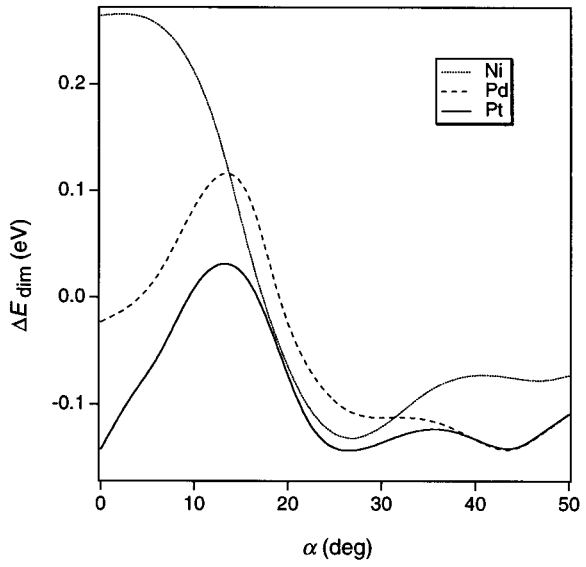

Figure 10. Dimerization energy, ΔE_{dim}, of $M(dmit)_2$ (M = Ni, Pd, Pt) units in the slipped configuration **7** and at the interplanar distance of 3.5 Å as a function of the slipping angle α.

As for the folded configuration, from Figure 9, where the dimerization energies are plotted as a function of the M−M distance, it is clear that the addition of one electron not only shifts all curves to lower energies with respect to the neutral free monomers but, more importantly, induces a flattening of the ΔE_{dim} well and a shift of the ΔE_{dim} minimum to longer M−M distance. The reason is that in the monoanionic dimers the intradimer bond is weaker than in the neutral ones at short M−M distances (2.5−3.1) due to the partial loss of the $4b_{1u} + 4b_{1u}$ electron pair bond but slightly stronger at long M−M distances due to the partial occupation of the $LUMO^+$ bonding orbital. The curves of Figure 9 indicate however that, in spite of the decrease of attractive orbital interaction energy, Pd and particularly Pt still form stable $[M(dmit)_2]_2^-$ dimers in the folded configuration, in agreement with the experimental findings according to which the charge transfer salts $[donor]_x[M(dmit)_2]_2$ (M = Pd, Pt; $0 < x < 1$) form stack structures containing folded dimers. It is worth noting, furthermore, that also the optimal M−M distances of ∼2.9 Å and ∼3.0 Å computed for the Pt and Pd dimers, respectively, fit in nicely with the average of the experimental values.

Electronic Structure and Bonding in the Slipped $[M(dmit)_2]_2^n$ ($n = 0, -1$) Dimers

Slipping is an efficient way to relieve the repulsions between adjacent $M(dmit)_2$ units and could be in principle preferred to the folding. As a matter of fact, in all $[donor]_x[Ni(dmit)_2]$ charge transfer salts[3−6] as well as in the neutral $[Ni(dmit)_2]$,[6f] the adjacent $Ni(dmit)_2$ units adopt invariably a slipped configuration. Therefore, with the aim to verify whether a slipped configuration may compete in stability with the metal-over-metal folded one, we have extended our theoretical investigation to $[M(dmit)_2]^n$ ($n = 0, -1$; M = Ni, Pd, Pt) dimers in the slipped configurations **7**−**9** (the monomers are kept planar).

One can figure out the main features of the electronic structure of the slipped dimers by considering how the relevant interactions occurring in the eclipsed dimers in configuration **5** change upon slipping. For a fixed interplanar distance, the slipping from the eclipsed stacking, be it along the *x* axis and the *y* axis or along the $M-S_1$ bond direction, produces an overall decrease of the intermolecular overlaps. The consequence is that both the attractive and repulsive (four-electron two-orbital) interactions will be reduced upon slippage. We will consider $[M(dmit)_2]_2$ dimers in which the slipped monomeric units are placed at the interplanar distance of 3.5 Å, that is the optimal theoretical value (when the $M(dmit)_2$ units approach closer than 3.5 Å a stable dimer is not being formed, whatever the slipping angle is), and corresponds fairly well to the average of the interplanar distances between adjacent monomeric units in the neutral $[Ni(dmit)_2]$,[6f] in most of the $[donor]_x[Ni(dmit)_2]$ charge transfer salts[3−6] as well as in α-TTF$[Pd(dmit)_2]_2$.[3b]

We find that, upon slipping along the *x* axis, the $HOMO^+$/$HOMO^-$ and $LUMO^+$/$LUMO^-$ splittings, which are already quite small in the eclipsed configuration at this distance, become so small that the two electron pair bonds are not being formed in $[Ni(dmit)_2]_2^n$ ($n = 0, -1$) dimers. The highest fully occupied molecular orbital is invariably the $HOMO^-$. In Pd and Pt dimers, owing to a smaller HOMO−LUMO gap, the two electron pair bonds are still formed at slipping angles <16°. Due to overlap reasons the splitting of the HOMO and LUMO decreases less rapidly with the slipping angle when the slippage occurs along the *y* axis. Our calculations indicate that the two electron pair bonds are still formed at slipping angles <20° in Pd and Pt and at slipping angles <16° in Ni dimers. In the case of slippage along the $M-S_1$ bond direction, the electron pair bonds are being formed only at very small slipping angles, i.e. smaller than 10°. As expected, the metal−metal σ interaction and the metal to ligand charge transfer, which, at the interplanar distance we are considering, were already weak in the eclipsed dimers, are almost completely lost upon slippage, particularly in Ni. Thus, apart from the electron pair bonds that at small slipping angles are still formed, two slipped $M(dmit)_2$ units are held together by many weak charge transfer and polarization interactions.

Looking at the ΔE_{dim} curves relative to the slipped configurations **7** shown in Figure 10, we note that in all dimers of the series the dimerization energy reaches a minimum when the slipping angle is ∼27°; i.e. when one S_1 atom in one $M(dmit)_2$ unit is equidistant from two S_1 atoms in the neighboring one. Past this point the ΔE_{dim} curves show small oscillations and a further minimum is found at ∼44° in Pd and Pt and at ∼48° in Ni. It should be noted however that the absolute value of the

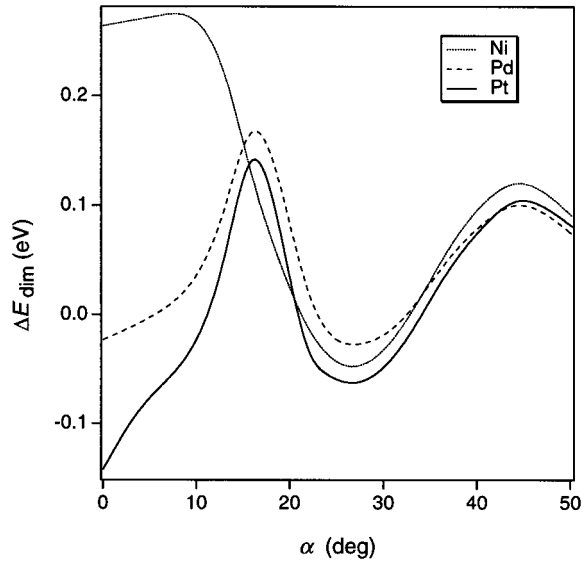

Figure 11. Dimerization energy, ΔE_{dim}, of $M(dmit)_2$ (M = Ni, Pd, Pt) units in the slipped configuration **8** and at the interplanar distance of 3.5 Å as a function of the slipping angle α.

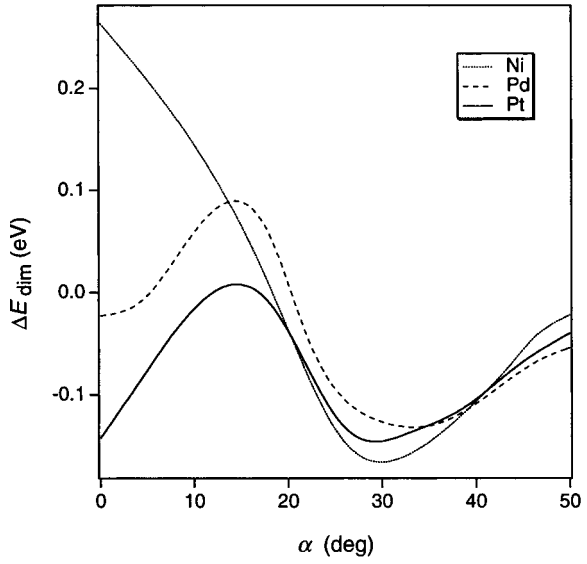

Figure 12. Dimerization energy, ΔE_{dim}, of $M(dmit)_2$ (M = Ni, Pd, Pt) units in the slipped configuration **9** and at the interplanar distance of 3.5 Å as a function of the slipping angle α.

dimerization energy changes very little in the range 27−50°, suggesting that $[M(dmit)_2]_2$ dimers with slippage angles within this range would be stable as well. Support for these findings comes from the reported structure of the neutral $[Ni(dmit)_2]$,[6f] where the $Ni(dmit)_2$ units are slipped along the *x* axis by an angle of 48°.

At slipping angles smaller than 27° the ΔE_{dim} curves of the three dimers differ significantly. In fact, the Ni curve increases monotonically toward 0°, whereas the Pd and Pt ones show a maximum at α ∼15°. The overall behavior of the dimerization energy as a function of the slipping angle along the $[M(dmit)_2]_2$ series can be understood with the help of a quantitative energy analysis (not reported here) of the contributions to the dimerization energies. This analysis indicates that the ΔE_{oi} term from 15° upward has a constant value of ∼−0.7 eV in all dimers and that it is the ΔE^0 term that controls the variation of the dimerization energy with the slipping angle. The minimum in the energy curves corresponds indeed to a slipping angle at which the ΔE^0 term reaches its lowest (least positive) value,

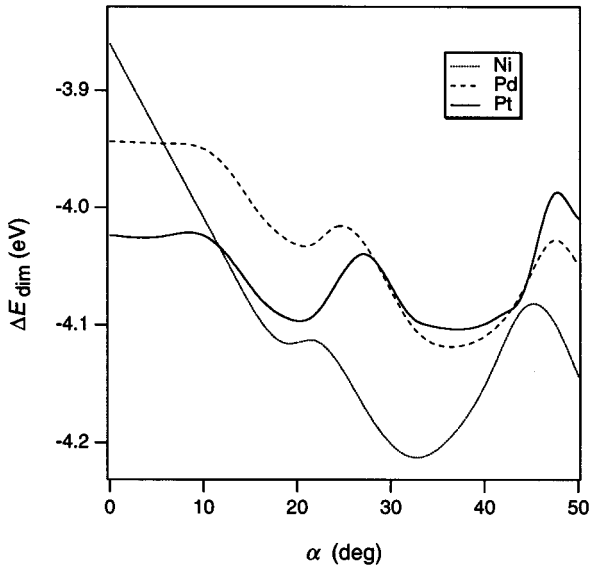

Figure 13. Dimerization energy, ΔE_{dim}, of $[M(dmit)_2]_2$ (M = Ni, Pd, Pt) units in the slipped configuration **7** and at the optimal interplanar distance of 3.5 Å as a function of the slipping angle α.

i.e. at which the Pauli repulsion is minimized. When the slipping angle decreases from 15 to 0°, the energy behaves rather differently in the case of Ni (increase) and Pd and Pt (decrease). The steric repulsions are not very different for the three cases. However, the excitation energy to bring the monomers in the right electronic configuration for the formation of the electron pair bonds is relatively large in $Ni(dmit)_2$ (1.2 eV *versus* 0.94 and 0.97 for Pd and Pt, respectively), while the electron pair bonds are not stronger for $Ni(dmit)_2$ (they are clearly stronger in Pt). These rather subtle energy differences make the eclipsed conformation unfavorable for Ni but tip the balance in favor of eclipsed conformation for Pt.

The same considerations hold for the variation of the energy as a function of the slipping angle α in the slipping directions **8** and **9**; see Figures 11 and 12. As inferred indeed from Figure 11, the ΔE_{dim} curves for the slipped configurations **8** show, as for the configuration **7**, a minimum at α ∼27°, i.e. when one S_1 atom in one $M(dmit)_2$ unit is equidistant from two S_1 atoms in the neighboring one. We note however that (i) the minimum in the dimerization energy at the optimal slipping angle is somewhat less deep than in the case of configuration **7** and (ii) past the minimum the dimerization energy rapidly becomes positive. These features of the ΔE_{dim} curves clearly indicate that the slipping along the *y* axis (**8**) is less favorable than the slipping along the *x* axis (**7**) and that slipping angles out of the range 22−32° are not compatible with stable $[M(dmit)_2]_2$ dimers in the slipped configuration **8**.

According to the ΔE_{dim} curves displayed in Figure 12, for the configuration **9** a minimum is found at α ∼30°, i.e. when the metal atom in one $M(dmit)_2$ unit lies over the S_1 atom in the neighboring one. Past the minimum the energy increases, but as in the case of the configuration **7**, it remains negative, indicatging that slipping angles larger than 30° may be adopted by the $[M(dmit)_2]_2$ dimers in the configuration **9**.

Coming to the monoanionic $[M(dmit)_2]_2$ dimers, from Figures 9 and 13, where the dimerization energies computed for the configurations **6** (eclipsed, folded) and **7** (slipped, unfolded) of the $[M(dmit)_2]_2^-$ dimers are reported, it is inferred that the relative stabilities of these two configurations are substantially the same as in the neutral dimers.

Concluding Remarks

The bonding between two M(dmit)$_2$ monomers (M = Ni, Pd, Pt) in the stacks that are characteristic for the crystal structure of these compounds has been analyzed, using decomposition of the interaction energy in Pauli repulsion and electrostatic attraction (together steric repulsion), electron pair bond formation, and donor−acceptor interactions.

Our analysis shows that the atom-over-atom (eclipsed) stacking may occur if two conditions are met: (i) The HOMO → LUMO excitation energy should be small enough so that these singly occupied ligand orbitals may both form an electron pair bond with their partner on the adjacent monomer. (ii) The bending away of the ligand systems so as to relieve the steric hindrance should not cost too much energy. These circumstances prevail in Pt(dmit)$_2$, where relativistic effects increase the stability of the eclipsed conformation by enhancing the metal−metal donor−acceptor interactions. In Ni(dmit)$_2$ both the excitation energy is somewhat higher and the bending is more unfavorable. Pd(dmit)$_2$ is in between. Slipping is another efficient way to relieve the steric repulsion between adjacent monomers. The electron pair bonds are broken in this case, but sufficient donor−acceptor interactions remain to make the slipped arrangement a viable alternative for Pd(dmit)$_2$ and Ni(dmit)$_2$.

When the relative stabilities of the unfolded slipped and metal-over-metal folded configurations of the [M(dmit)$_2$]$_2$ dimers are compared, it appears that (i) the metal-over-metal folded configuration **6** is by far the preferred one for Pt dimers, (ii) the metal-over-metal folded configuration **6** may compete energetically with any of the slipped configurations **7**−**9** in the case of Pd dimers, and (iii) any of the slipped configurations **7**−**9** is much more favorable than the metal-over-metal folded one in the case of Ni dimers.

These conclusions still hold when considering the monoanionic [M(dmit)$_2$]$_2$ dimers. Thus, in nice agreement with the experiments, our calculations predict that in the [donor]$_x$[M(dmit)$_2$] charge transfer salts the adjacent M(dmit)$_2$ units will adopt a slipped configuration in the case of Ni, a metal-over-metal folded configuration in the case of Pt, and either a slipped or a metal-over-metal folded configuration in the case of Pd.

We have then clearly identified electronic structural reasons as the origin of the different intrastack overlap modes shown by the three members of the series.

Acknowledgment. This work has been partially supported by the Italian National Research Council (CNR). A.R. gratefully acknowledges a grant from the European Science Foundation (ESF) in the framework of the "Relativistic Effects in Heavy-Element Chemistry and Physics" (REHE) Programme. A grant of computation time by the foundation Nationale Computer Faciliteiten (NCS) of the Netherlands Organization for Scientific Research (NWO) is gratefully acknowledged.

IC970452L